

finite sequence S of m query-points is given by

$$O\left(\mathcal{F}(\mathcal{T}) \cdot \sum_{i=1}^m |e_i|\right) + O(m) \quad (1)$$

where e_i is the line segment formed by the i -th starting point and the i -th query-point. The $O(m)$ expression in Eq.(1) appears because answering one query costs at least $O(1)$. Since the only points we can use as starting points for next locations are points that we know where they are, the line segments $(e_i)_{1 \leq i \leq m}$ must be connected. Therefore the graph \mathcal{E} formed by these line segments is a tree spanning the query-points; such a tree is called the *Location Tree* in the sequel. Its length is given by:

$$|\mathcal{E}| = \sum_{e_i \in \mathcal{E}} |e_i|.$$

Note that the Location Tree might have vertices which do not belong to S .

2.3 On Trees Embedded in \mathbb{R}^d

The tree theory is older than computational geometry itself. Here, we mention some of the well-known trees [22] which are related with the theory of point location. Let $S = \{x_i, 1 \leq i \leq n\}$ be a set of query-points in \mathbb{R}^d and $G = (V, E)$ be the complete graph such that the vertex $v_i \in V$ is embedded on the point $x_i \in S$; the edge $e_{ij} \in E$ linking two vertices v_i and v_j is weighted by its Euclidean length $|x_i - x_j|$. G is usually referred to as the *geometric graph* of S .

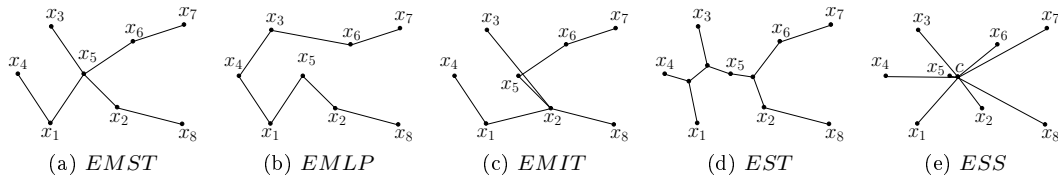


Figure 2: Trees and graphs embedded in \mathbb{R}^d .

2.3.1 Definitions

We review below some well-known trees. Two special kinds of tree get a special name: (i) a *star* is a tree having one vertex that is linked to all others; and (ii) a *path* is a tree having all vertices of degree 2 but two with degree 1.

EMST. Among all the trees spanning S , a tree with the minimal length is called an *Euclidean minimum spanning tree* of S and denoted $EMST(S)$, see Figure 2a. $EMST$ can be computed with a greedy algorithm at a polynomial complexity.

EMLP. If instead of searching a tree, we search a path with minimal length spanning S , we get the *Euclidean minimum length path* denoted by $EMLP(S)$, see Figure 2b. Another related problem is the search for a minimal tour spanning S : the *Euclidean traveling salesman tour*, denoted by $ETST$. Both problems are NP-complete.

Since a complete traversal of the *EMST* (either prefix, infix or postfix) produces a tour, and removing an edge of *ETST* produces a path, we have

$$|EMST(S)| \leq |EMLP(S)| < |ETST(S)| < 2|EMST(S)| \quad (2)$$

EMIT. Above, subgraphs of G are independent of any ordering of the vertices. Now, consider that an ordering is given by a permutation σ , vertices are inserted in the order $v_{\sigma(1)}, v_{\sigma(2)}, \dots, v_{\sigma(n)}$. We build incrementally a spanning tree T_i for $S_i = \{x_{\sigma(j)} \in S, i \leq j\}$ with $T_1 = \{v_{\sigma(1)}\}$ and $T_i = T_{i-1} \cup \{v_{\sigma(i)}v_{\sigma(j)}\}$, such that $v_{\sigma(i)}v_{\sigma(j)}$ has the shortest length for any $1 \leq j < i$. This tree is called the *Euclidean minimum insertion tree*, and will be denoted by $EMIT(S)$, see Figure 2c. Unlike the previous trees, *EMIT* does not require points to be known in advance, and hence it is a dynamic structure. Its length depends on σ and for some carefully chosen permutations it coincides with $|EMST|$.

EST. The use of additional vertices usually allows to decrease the length of a tree. Such additional vertices are called *Steiner points* and the minimum-length tree with Steiner points is the *Euclidean Steiner tree* of S ; it is denoted by $EST(S)$, see Figure 2d. Finding *EST* is NP-complete.

ESS. A star has one vertex linked to all other vertices. If this vertex is an additional vertex that does not belong to V , we can choose its position so as to minimize the length of the star. This point is called the *Fermat-Weber point* of S and the associated star is denoted by $ESS(S)$ (*Euclidean Steiner star*), see Figure 2e.

2.3.2 Results on Tree's Length.

We present here some results on the length of the above-mentioned structures. We start by the static setting, involving subgraphs which are independent of an ordering of the vertices. The Beardwood, Halton and Hammersley theorem [4] states that if x_i are i.i.d. random variables with compact support, then $|ETST(S)| = O(m^{1-1/d})$ with probability 1. By Eq.(2) the same bound is obtained for $|EMLP(S)|$ and $|EMST(S)|$. While this result gives a practical bound on the complexity, they are dependent on probabilistic hypotheses. This was shown to be unnecessary. Steele proves [24] that the complexity of these graphs remains bounded by $O(m^{1-1/d})$ even in the worst case.

Consider the length of the path formed by sequentially visiting each vertex in V . This gives a total length of $\sum_{i=2}^m |x_{i-1}x_i|$. Let $V_\sigma = \{x_{\sigma(1)}, x_{\sigma(2)}, \dots, x_{\sigma(m)}\}$ be a sequence of m points made by reordering V with a permutation function σ such that points in V_σ would appear in sequence on some *space-filling* curve. Platzman and Bartholdi [19] proved that in two dimensions the length of the path made by visiting S_σ sequentially is a $O(\log m)$ approximation of $|ETST(S)|$, and hence $\sum_{i=2}^m |x_{\sigma(i-1)}x_{\sigma(i)}| = O(\sqrt{m} \log m)$. One of the main interests of such heuristic is that σ can be found in $O(m \log m)$ time.

The asymptotic length of $|EMIT(S)|$, which is dynamic, is shown to be the same as the one of $|EMST(S)|$, which is static. This result is surprising because it means that replacing a dynamic setting by a static setting does not affect the asymptotic length of trees following the greedy strategy of an *EMST*. More precisely:

Theorem 2 (Steele [23]). *Let S be a sequence of m points in $[0, 1]^d$, $d \geq 2$, then $|EMST(S)| \leq |EMIT(S)| \leq \gamma_d m^{1-1/d}$. Here, $\gamma_d = 1 + 2^{4d} d^{d/2} / (d-1)$ is a constant depending only on d .*

3 Constant Size Memory Strategies

Let S be a sequence of m query-points in \mathcal{C} to be located in a triangulation satisfying the Distribution Condition with $\mathcal{F}(\mathcal{T}) \gg 1$. In this section, we analyze the cost of strategies that store a constant number of possible starting points for a straight-walk. We also provide a comparative study between them.

3.1 Fixed-point strategy.

In the fixed-point strategy, the same point c is used as starting point for all the queries, then the Location Tree is the star rooted at c , denoted by $S_c(S)$. The best Location Tree we can imagine is the Steiner star, but of course computing it is not an option neither in a dynamic setting nor in a static setting. This strategy is used in practice: In CGAL 3.5, the default starting point for a walk is the so-called *vertex at infinity*; thus the walk starts somewhere on the convex hull, which looks like a kind of worst strategy.

In the worst case, one can easily find a set of query-points S such that $|ESS(S)| = O(m)$, or such that $|S_c(S)|/|ESS(S)|$ goes to infinity for some c . Now we focus on the case of evenly distributed queries.

Theorem 3. *When query-points in S are uniformly i.i.d in a ball, and \mathcal{T} satisfies the Distribution Condition, the expected cost of the best fixed-point strategy is*

$$\left(\frac{d}{d+1}\right) m \mathcal{F}(\mathcal{T}).$$

Proof. By symmetry, the Fermat-Weber point goes to the center of the circle when m goes to infinity, thus we evaluate the average length $E(|Op|)$ between a random point p and the origin. Let \mathcal{B}_l be a ball with radius l centered at the origin, we have

$$E(|Op|) = \int_0^1 l \text{Prob}(p \in \mathcal{B}_{l+d} \setminus \mathcal{B}_l) = \int_0^1 l \frac{(dV_d(l)/l)dl}{V_d(1)} = \int_0^1 dl^d = \frac{d}{d+1},$$

where $V_d(l)$ is the volume of a ball of radius l (and $dV_d(l)/l$ is its area). Multiplying by m gives the expected length of the Location Tree, multiplying by $\mathcal{F}(\mathcal{T})$ using the Distribution Condition ends the proof. \square

Theorem 4. *When query-points in S are uniformly i.i.d in a ball, and \mathcal{T} satisfies the Distribution Condition, the expected cost of the worst (on the choice of c inside the ball) fixed-point strategy is*

$$2^{d+1} \left(\frac{2d+1}{2d+2}\right) \frac{B\left(\frac{d}{2} + \frac{1}{2}, \frac{d}{2} + 1\right)}{B\left(\frac{d}{2} + \frac{1}{2}, \frac{1}{2}\right)} m \mathcal{F}(\mathcal{T}),$$

where $B(x, y) = \int_0^1 \lambda^{x-1}(1-\lambda)^{y-1}d\lambda$ is the so-called Beta function.

By symmetry, any point on the boundary of the unit sphere is a worse center for a star. The computation of the average is a bit more involved than in Theorem 3, and we split the computation in several lemmas.

Lemma 5. Consider the spherical cap \mathcal{H}_h formed by crossing a ball \mathcal{B}_R with radius R centered at the origin, with the plane $x = R - h$. Denote h the height of the cap. The volume of \mathcal{H}_h is the volume of the intersection between the half-space $x \geq R - h$ and \mathcal{B}_R . This volume is given by:

$$R^d \frac{\pi^{\frac{d-1}{2}}}{\Gamma(\frac{d+1}{2})} \int_0^{\arccos(\frac{R-h}{R})} \sin^d(\lambda) d\lambda. \quad (3)$$

Proof. The volume $V_d(r)$ of a ball with radius r in dimension d is given by $r^d \cdot \pi^{\frac{d}{2}} / \Gamma(1 + \frac{d}{2})$. Each cross-section $x = R - h + \delta$, $0 \leq \delta \leq h$ is a $(d-1)$ -dimensional ball. If we integrate all those balls along the x axis, we have $\int_{R-h}^R V_{d-1}(\sqrt{R^2 - t^2}) dt$. Eq. (3) follows from replacing t by $\lambda = R \cos(t)$. \square

Lemma 6. Let Ω be a point on the boundary of the unit ball \mathcal{B}_{unit} , and $P_{\mathcal{H}}(l) = \text{Prob}(|\Omega p| \leq l; p \in \mathcal{B}_{unit})$ be the cumulative distribution function of distances between an uniformly distributed random point inside \mathcal{B}_{unit} and Ω , then

$$P_{\mathcal{H}}(l) = \frac{1}{B(\frac{d}{2} + \frac{1}{2}, \frac{1}{2})} \left(\int_0^{\arccos(1-l^2/2)} \sin^d(\lambda) d\lambda + l^d \int_0^{\arccos(l/2)} \sin^d(\lambda) d\lambda \right),$$

where $B(x, y) = \int_0^1 \lambda^{x-1} (1-\lambda)^{y-1} d\lambda$ is the Beta function.

Proof. If we denote \mathcal{B}_l the ball of radius l centered in Ω , the desired probability is clearly $\text{volume}(\mathcal{B}_l \cap \mathcal{B}_{unit}) / \text{volume}(\mathcal{B}_{unit})$. $\mathcal{B}_l \cap \mathcal{B}_{unit}$ is the union of two spherical caps limited by the plane $x = 1 - l^2/2$ which can be computed using Lemma 5. \square

Proof of Theorem 4. The theorem follows from:

$$\begin{aligned} E\{|\Omega p|\} &= \int_0^2 l P'_{\mathcal{H}}(l) dl \\ &= \int_0^2 l \left(\frac{\frac{1}{2} l^d \left(1 - \frac{l^2}{4}\right)^{\frac{d-1}{2}}}{B(\frac{d}{2} + \frac{1}{2}, \frac{1}{2})} + dl^{d-1} \frac{\int_0^{\arccos(l/2)} \sin^d(\lambda) d\lambda}{B(\frac{d}{2} + \frac{1}{2}, \frac{1}{2})} \right) dl \\ &= \frac{1}{2} \int_0^2 \frac{l^{d+1} \left(1 - \frac{l^2}{4}\right)^{\frac{d-1}{2}}}{B(\frac{d}{2} + \frac{1}{2}, \frac{1}{2})} dl + \frac{1}{2} \int_0^2 \frac{2dl^d \int_0^{\arccos(l/2)} \sin^d(\lambda) d\lambda}{B(\frac{d}{2} + \frac{1}{2}, \frac{1}{2})} dl \end{aligned} \quad (4)$$

The right part of Expression (4) corresponds exactly to the expected value of l where l is a random segment determined by two evenly distributed points in the unit ball [21]. Its value is given by:

$$\int_0^2 \frac{2dl^d \int_0^{\arccos(l/2)} \sin^d(\lambda) d\lambda}{B(\frac{d}{2} + \frac{1}{2}, \frac{1}{2})} dl = 2^{d+1} \left(\frac{d}{d+1} \right) \frac{B(\frac{d}{2} + \frac{1}{2}, \frac{d}{2} + 1)}{B(\frac{d}{2} + \frac{1}{2}, \frac{1}{2})}. \quad (5)$$

The left part of Expression (4) can be obtained as follows:

$$\begin{aligned}
\int_0^2 \frac{l^{d+1} \left(1 - \frac{l^2}{4}\right)^{\frac{d-1}{2}} dl}{B\left(\frac{d}{2} + \frac{1}{2}, \frac{1}{2}\right)} &= 2 \int_0^1 \frac{2^{d+1} y^{d+1} (1 - y^2)^{\frac{d-1}{2}} dy}{B\left(\frac{d}{2} + \frac{1}{2}, \frac{1}{2}\right)} \\
&= \int_0^1 \frac{2^{d+1} z^{\frac{d}{2}} (1 - z)^{\frac{d-1}{2}} dz}{B\left(\frac{d}{2} + \frac{1}{2}, \frac{1}{2}\right)} \\
&= 2^{d+1} \frac{B\left(\frac{d}{2} + \frac{1}{2}, \frac{d}{2} + 1\right)}{B\left(\frac{d}{2} + \frac{1}{2}, \frac{1}{2}\right)}.
\end{aligned}$$

Finally, we have

$$E\{|\Omega p|\} = 2^{d+1} \left(\frac{2d+1}{2d+2}\right) \frac{B\left(\frac{d}{2} + \frac{1}{2}, \frac{d}{2} + 1\right)}{B\left(\frac{d}{2} + \frac{1}{2}, \frac{1}{2}\right)}.$$

Multiplying by m gives the expected length of the Location Tree, multiplying by $\mathcal{F}(\mathcal{T})$ using the Distribution Condition ends the proof. \square

Corollary 7. *When query-points in S are uniformly i.i.d in a ball, and \mathcal{T} satisfies the Distribution Condition, the ratio between the costs of the best and worst fixed-point strategies is at most 2 (for $d = 1$), and at least $\sqrt{2}$ (when $d \rightarrow \infty$).*

Proof. This ratio is a decreasing function of the dimension, basic computations on Beta functions gives the value for $d = 1$ and $d = \infty$.

Using Theorem 3 and Theorem 4, the ratio $\rho(d)$ between the costs of the worst and the best fixed-point strategies is given by:

$$\rho(d) = 2^{d+1} \left(\frac{2d+1}{2d}\right) \frac{B\left(\frac{d}{2} + 1, \frac{d}{2} + \frac{1}{2}\right)}{B\left(\frac{d+1}{2}, \frac{1}{2}\right)}$$

Since $\rho(d)$ is a monotonic decreasing function, its extremal values are $\rho(1)$ and $\lim_{d \rightarrow \infty} \rho(d)$. We have trivially from Eq.(3.1) that $\rho(1) = 2$. To prove Corollary 7, it remains to find $\lim_{d \rightarrow \infty} \rho(d)$. Using the Stirling's identities:

$$\begin{aligned}
B(a, b) &\sim \sqrt{2\pi} \frac{a^{a-\frac{1}{2}} b^{b-\frac{1}{2}}}{(a+b)^{a+b-\frac{1}{2}}}, & a, b \gg 0, \\
B(a, b) &\sim \Gamma(b) a^{-b}, & a \gg b > 0,
\end{aligned}$$

we have:

$$\begin{aligned}
\lim_{d \rightarrow \infty} \rho(d) &= \lim_{d \rightarrow \infty} 2^{d+1} \left(\frac{2d+1}{2d} \right) \frac{B\left(\frac{d}{2}+1, \frac{d}{2}+\frac{1}{2}\right)}{B\left(\frac{d+1}{2}, \frac{1}{2}\right)} \\
&= \lim_{d \rightarrow \infty} 2^{d+1} \frac{B\left(\frac{d}{2}+1, \frac{d}{2}+\frac{1}{2}\right)}{B\left(\frac{d+1}{2}, \frac{1}{2}\right)} \\
&= \lim_{d \rightarrow \infty} \frac{2^{d+1} \sqrt{2\pi} \left(\frac{d}{2}+\frac{1}{2}\right)^{\frac{d}{2}} \left(\frac{d}{2}+1\right)^{\frac{d}{2}+\frac{1}{2}}}{\sqrt{\pi} \left(d+\frac{3}{2}\right)^{d+1} \left(\frac{d}{2}+\frac{1}{2}\right)^{-\frac{1}{2}}} \\
&= 2^{1/2} \cdot \lim_{d \rightarrow \infty} \frac{(d+1)^{\frac{d+1}{2}} (d+2)^{\frac{d+1}{2}}}{\left(d+\frac{3}{2}\right)^{\frac{d+1}{2}} \left(d+\frac{3}{2}\right)^{\frac{d+1}{2}}} \\
&= 2^{1/2} \cdot e^{-\frac{1}{4}} \cdot e^{\frac{1}{4}} \\
&= \sqrt{2}
\end{aligned}$$

Then we have that $\sqrt{2} \leq \rho(d) \leq 2$ for $d \geq 1$. \square

Figure 3 gives the expected average length of an edge of the best and worst fixed-point Location Trees.

3.2 Last-point strategy.

An easy alternative to the fixed-point strategy is the last-point strategy. To locate a new query-point, the walk starts from the previously located query. The Location Tree obtained with such a strategy is a path. When \mathcal{T} verifies the Distribution Condition, the optimal path is the $EMLP(S)$.

In the worst case the length of such a path is clearly $O(m)$, an easy example is to repeat alternatively the two same queries. In contrast with the fixed-point strategy, the last-point strategy depends on the queries distribution. If the queries have some spatial coherence, it is clear that we improve on the fixed-point strategy. Such a coherence may come from the application, or by reordering the queries. There is always a permutation of indices on S such that the total length of the path is sub-linear [24, 12]. Furthermore, in two dimensions, one could find such permutation in $O(m \log m)$ time complexity [19].

Now, the question is ‘‘if there is no spatial coherence, how the fixed and last point strategies do compare?’’.

Theorem 8. *When \mathcal{T} satisfies the Distribution Condition, then the fixed-point strategy cannot improve the last-point strategy by a factor bigger than 2.*

Proof. This is an easy consequence of the triangle inequality.

Take $S = x_1, x_2, \dots, x_m$, and any fixed-point c . Then we have:

$$|x_i x_{i+1}| \leq |cx_i| + |cx_{i+1}|,$$

for all $1 \leq i < m$. Summing the term above for each value of i leads to the inequality:

$$\sum_{i=1}^{m-1} |x_i x_{i+1}| \leq \sum_{i=1}^{m-1} |cx_i| + \sum_{i=2}^m |cx_i| \leq 2 \sum_{i=1}^m |cx_i|.$$

Multiplying each side by $\mathcal{F}(\mathcal{T})$ completes the proof. \square

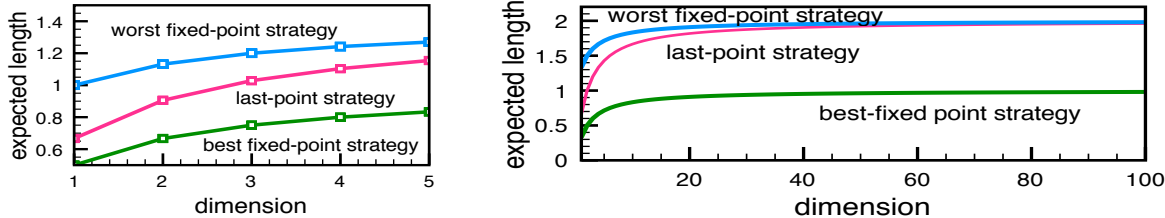


Figure 3: **Expected lengths.** Expected average lengths of an edge of the last-point, best and worst fixed-point Location Trees. The domain \mathcal{C} here is a d -dimensional ball, and the queries are evenly distributed in \mathcal{C} .

Theorem 9. *When \mathcal{T} satisfies the Distribution Condition, then the last-point strategy can improve the fixed-point strategy by an arbitrarily large factor.*

Proof. Consider a set of m queries distributed on a circle in \mathbb{R}^d . If the queries are visited along the circle, the length of the location tree of the last-point strategy is $O(1)$, while $|ESS| = O(m)$. \square

Combining the results in Theorem 8 and Theorem 9, it is reasonable to conclude that the last-point strategy is better in general, as the improvement the fixed-point strategy could bring does not pay the price of its worst-case behavior. We now study the case of evenly distributed queries.

Theorem 10. *When query-points in S are uniformly i.i.d in a ball, and \mathcal{T} satisfies the Distribution Condition, the expected cost of the last-point strategy is*

$$2^{d+1} \left(\frac{d}{d+1} \right) \frac{B\left(\frac{d}{2} + \frac{1}{2}, \frac{d}{2} + 1\right)}{B\left(\frac{d}{2} + \frac{1}{2}, \frac{1}{2}\right)} m\mathcal{F}(\mathcal{T}).$$

Proof. This is equivalent to find the expected length of a random segment determined by two evenly distributed points in the unit ball, which is given in [21] for instance. \square

Theorems 3, 4, and 10 give the following result:

Corollary 11. *When query-points in S are uniformly i.i.d in a ball, and \mathcal{T} satisfies the Distribution Condition, the ratio between the costs of the last-point and the best fixed-point strategies is at most $\sqrt{2}$ (when $d \rightarrow \infty$), and at least $4/3$ (when $d = 1$) whereas the ratio between the costs of the last-point and the worst fixed-point strategies is $2d/(2d+1)$.*

As shown in Figure 3, the last-point strategy is in between the best and worst fixed-point strategies, but closer and closer to the worst one when d increases. Thus in the context of evenly distributed points in a ball, the last-point strategy cannot be worse than any fixed point strategy by more than a factor of $\sqrt{2}$. Still, the fixed-point strategy may have some interests under some conditions: (i) queries are known *a priori* to be random **and**; (ii) a reasonable approximation of the center of $ESS(S)$ can be found.

Theorem 10 and Corollary 11 assume that \mathcal{C} is a ball. Now, one might ask whether the shape of \mathcal{C} affects the cost of the strategies. In the quest for an

answer, we may consider query-points uniformly i.i.d in the unit cube $[0, 1]^d$. This leads to the following related expressions:

$$\begin{aligned} B_d &= \int_0^1 \dots \int_0^1 (\lambda_1^2 + \dots + \lambda_d^2)^{1/2} d\lambda_1 \dots d\lambda_d, \\ \Delta_d &= \int_0^1 \dots \int_0^1 ((\lambda_1 - \lambda'_1)^2 + \dots + (\lambda_d - \lambda'_d)^2)^{1/2} d\lambda_1 \dots d\lambda_d d\lambda'_1 \dots d\lambda'_d, \\ X_d &= \int_0^1 \dots \int_0^1 ((\lambda_1 - 1/2)^2 + \dots + (\lambda_d - 1/2)^2)^{1/2} d\lambda_1 \dots d\lambda_d, \end{aligned}$$

where B_d , X_d , and Δ_d are respectively the average length of an edge of: the smallest star (rooted at the center), the largest star (rooted at a corner), and of a random path. Above expressions are often referred to as *box integrals* [3]. First, note that by substitution of variable we have $B_d/X_d = 2$, independently of d . In Anderssen *et al.* [20], we have that, $X_d \sim \sqrt{d/3}$ and $\Delta_d \sim \sqrt{d/6}$ and thus B_d/Δ_d and $\Delta_d/X_d \sim \sqrt{2}$ when d goes to infinity. These ratios have to be compared with Corollary 7. If \mathcal{C} is an unit cube the costs of the last-point, best and worst fixed-point strategies remains in bounded ratio, but with different values compared to the case where \mathcal{C} is a ball. Notice however that the ratio between the best fixed-point and the last-point strategies remains $\sqrt{2}$ in both cases when d is large. This ratio in some sense is more robust than the ratios involving the worst-case fixed-point strategy.

3.3 k -last-points strategy.

We explore here a variation of the last-point strategy. Instead of remembering the place where the last query was located, we store the places where the k last queries were located, for some small constant k . These k places are called *landmarks* in what follows. Then to process a new query, the closest landmarks are determined by $O(k)$ brute-force comparisons, then a walk is performed from there. This strategy has some similarity with Jump & Walk, the main differences are that the sample has fixed size and depends on the queries distribution (it is dynamically modified).

The Location Tree associated with such a strategy has bounded degree $k+1$ (or the *kissing number* in dimension d , if it is smaller than $k+1$) and its length is greater than $|EMST|$ and smaller than the length of the path associated to the same vertices ordering, thus previous results provide upper and lower bounds. A tree of length $O(m/k) = O(m)$ is easily achieved by repeating a sequence of k queries along a circle of length 1. The following Theorem gives the complexity when the queries are evenly distributed:

Theorem 12. *When query-points in S are uniformly i.i.d in a ball, and \mathcal{T} satisfies the Distribution Condition, the expected cost of the k -last-points strategy verifies*

$$\left(\frac{1}{d}\right) B \left(k+1, \frac{1}{d}\right) m\mathcal{F}(\mathcal{T}) \leq E(\text{cost}) \leq 2 \left(\frac{1}{d}\right) B \left(k+1, \frac{1}{d}\right) m\mathcal{F}(\mathcal{T}), \quad (6)$$

First we will evaluate the distance between the origin and the closest amongst k points $\{p_1, p_2, \dots, p_k\}$ evenly distributed in the unit ball.

Lemma 13. *Let $P_{\mathcal{B},k}(l) = \text{Prob}(\min(|Op_j|)_{1 \leq j \leq k} \leq l)$ be the cumulative distribution function of the minimum distance among k points following a uniformly*

i.i.d inside the unit ball, and the center of the unit ball, then

$$P_{\mathcal{B},k}(l) = 1 - (1 - l^d)^k.$$

Proof.

$$\begin{aligned} P_{\mathcal{B},k}(l) &= \text{Prob}(\min(|Op_j|)_{1 \leq j \leq k} \leq l) \\ &= 1 - \text{Prob}(|Op_j| > l, 1 \leq j \leq k) \\ &= 1 - \text{Prob}(|Op_1| > l)^k \\ &= 1 - (1 - \text{Prob}(|Op_1| \leq l))^k \\ &= 1 - (1 - l^d)^k, \end{aligned}$$

since $\text{Prob}(|Op_1| \leq l)$ is the ratio of the ball of radius l over the unit ball. \square

Lemma 14. *The expected value $E(\min(|Op_j|)_{1 \leq j \leq k})$ of the minimum distance among k points following a uniformly i.i.d inside the unit ball and the center of the unit ball, is given by*

$$E(\min(|Op_j|)_{1 \leq j \leq k}) = \frac{1}{d} B\left(k+1, \frac{1}{d}\right).$$

Proof. Using Lemma 13, we have:

$$\begin{aligned} E(\min(|Op_j|)_{1 \leq j \leq k}) &= \int_0^1 l P'_{\mathcal{B},k}(l) dl \\ &= kd \int_0^1 l^d (1 - l^d)^{k-1} dl \\ &= k \int_0^1 \lambda^{1/d} (1 - \lambda)^{k-1} d\lambda \\ &= kB\left(k, 1 + \frac{1}{d}\right) = \frac{1}{d} B\left(k+1, \frac{1}{d}\right). \end{aligned}$$

\square

Lemma 14 gives us the lower-bound in Theorem 12. Now, we shall obtain the upper-bound, which is a bit more involved. First we will evaluate the distance between a point on the boundary and the closest amongst k points $\{p_1, p_2, \dots, p_k\}$ evenly distributed in the unit ball.

Lemma 15. *Let Ω be a point on the boundary of the unit ball and $P_{\mathcal{H},k}(l) = \text{Prob}(\min(|\Omega p_j|)_{1 \leq j \leq k} \leq l)$ be the cumulative distribution function of the minimum distance among k points following a uniformly i.i.d inside the unit ball, and Ω , then*

$$P_{\mathcal{H},k}(l) = 1 - (1 - P_{\mathcal{H}}(l))^k.$$

Proof.

$$\begin{aligned} P_{\mathcal{H},k}(l) &= \text{Prob}(\min(|\Omega p_j|)_{1 \leq j \leq k} \leq l) \\ &= 1 - \text{Prob}(|\Omega p_j| > l, 1 \leq j \leq k) \\ &= 1 - \text{Prob}(|\Omega p_1| > l)^k \\ &= 1 - (1 - \text{Prob}(|\Omega p_1| \leq l))^k, \end{aligned}$$

$P_{\mathcal{H}}(l)$ as given at Lemma 6. The exact expression of $P_{\mathcal{H},k}(l)$ is not necessary in the sequel. \square

Now, we shall obtain a general expression for the expected value of $\min(|\Omega p_j|)_{1 \leq j \leq k}$.

Lemma 16. *The expected value $E(\min(|\Omega p_j|)_{1 \leq j \leq k})$ of the minimum distance among k points following a uniformly i.i.d inside the unit ball and Ω , is given by*

$$E(\min(|\Omega p_j|)_{1 \leq j \leq k}) = \int_0^2 (1 - P_{\mathcal{H}}(l))^k dl.$$

Proof. As $P_{\mathcal{H}}(0) = 0$ and $P_{\mathcal{H}}(2) = 1$, integration by parts gives us the following identity:

$$\int_0^2 l P'_{\mathcal{H}}(l) P_{\mathcal{H}}^{i-1}(l) dl = \frac{2 - \int_0^2 P_{\mathcal{H}}^i(l) dl}{i}, i > 0. \quad (7)$$

We also have the following expression for $E(\min(|\Omega p_j|)_{1 \leq j \leq k})$:

$$\begin{aligned} E(\min(|\Omega p_j|)_{1 \leq j \leq k}) &= \int_0^2 k l P'_{\mathcal{H}}(l) (1 - P_{\mathcal{H}}(l))^{k-1} dl \\ &= \sum_{i=0}^{k-1} (-1)^i \binom{k-1}{i} \int_0^2 k l P'_{\mathcal{H}}(l) P_{\mathcal{H}}^i(l) dl. \end{aligned} \quad (8)$$

Replacing Eq. (7) in Eq. (8) leads to:

$$\begin{aligned} \sum_{i=0}^{k-1} (-1)^i \binom{k-1}{i} \int_0^2 k l P'_{\mathcal{H}}(l) P_{\mathcal{H}}^i(l) dl &= \sum_{i=0}^k (-1)^i \binom{k}{i} \int_0^2 P_{\mathcal{H}}^i(l) dl \\ &= \int_0^2 \sum_{i=0}^k (-1)^i \binom{k}{i} P_{\mathcal{H}}^i(l) dl \\ &= \int_0^2 (1 - P_{\mathcal{H}}(l))^k dl. \end{aligned}$$

\square

Proof of Theorem 12. Now, if we take a function $\Psi(l)$ such that $\Psi(l) \leq P_{\mathcal{H}}(l)$ for $0 \leq l \leq 2$, it upper-bounds the integral in Lemma 16. Take $\Psi(l) = (l/2)^d$, then we have:

$$\begin{aligned} E(\min(|\Omega p_j|)_{1 \leq j \leq k}) &= \int_0^2 (1 - P_{\mathcal{H}}(l))^k dl \leq \int_0^2 (1 - \Psi(l))^k dl \\ &= \int_0^2 \left(1 - \frac{l^d}{2^d}\right)^k dl \\ &= 2 \int_0^1 (1 - \lambda^d)^k d\lambda \\ &= 2 \left(\frac{1}{d}\right) \int_0^1 y^{(1/d)-1} (1 - y)^k dy \\ &= 2 \left(\frac{1}{d}\right) B\left(k+1, \frac{1}{d}\right). \end{aligned}$$

This completes the proof. \square

Remark: If we no longer consider k as a constant, then taking $k = m$ makes the Location Tree of the k -last-points strategy an *EMIT*. And hence, using the Stirling's identity $B(x, y) \sim \Gamma(y)x^{-y}$ in Eq.(6) gives an expected length $|EMIT| = \Theta(m^{1-1/d})$. Comparing to Theorem 2, the asymptotic growth in both random and worst case are the same, but the constant is much better in the random case. ■

Intuitively, if the queries have some not too strong spatial coherence, the k -last-points strategy seems a good way to improve the last-point strategy. Surprisingly, experiments in Section 6 shows that even if the points have some strong coherence, a small k strictly greater than 1 improves on the last-point strategy when points are sorted along a space-filling curve. More precisely, $k = 4$ improves the location time by up to 15% on some data sets.

4 Jump & Walk revisited: Keep, Jump & Walk

In this section, the k -last-points strategy is extended to a variable k . Here, it is necessary to have a closer look at the way of managing the landmarks. The classical Jump & Walk¹ strategy [11, 17] uses a set of k landmarks randomly chosen in the vertices of \mathcal{T} , then a query is located by walking from the closest landmark. To ensure adaptation of the query distribution we have several possibilities: (i) we can use k queries chosen at random in previous queries, (ii) we can use the k last queries for the set of landmarks, and (iii) we can keep all the queries as landmarks, and regularly clear the landmarks set after a batch of k queries.

For any rule to construct the set of landmarks, the time to process a query q splits in:

- Keep: the time $Q(k)$ for updating the set of landmarks if needed,
- Jump: the time $J(k)$ for finding the closest landmark l_q , and
- Walk: the time $|ql_q|\mathcal{F}(\mathcal{T})$ to walk in \mathcal{T} assuming that \mathcal{T} satisfies the Distribution Condition.

Combining various options for $\mathcal{F}(\mathcal{T})$ and the data structure to store the landmarks, gives us some interesting possibilities. The trick is always to balance these different costs, since increasing one decreases another.

Jump & Walk. Classical Jump & Walk uses a simple data structure (e.g. a list) to store the random sample of \mathcal{T} and assumes $\mathcal{F}(n) = O(n^{1/d})$. Here, we will use the same data structure to store the set of landmarks. Keep step decides whether the query is kept at a landmark and inserts it if needed. This takes $Q(k) = O(1)$. Jump step takes $J(k) = O(k)$. Then taking $k = n^{1/(d+1)}$ landmarks amongst the queries ensures an amortized query time of $O(n^{1/(d+1)})$ as $|ql_q| = O(k^{-1/d})$ by Theorem 2. It is noteworthy that the complexity obtained here matches the classical Jump & Walk complexity with no hypotheses on the distribution of query-points.

Outside this classical framework, Jump & Walk has some interests, even with weaker hypotheses. Theorem 2 ensures that $|ql_q|$ has amortized length

¹ Apropos, Jump & Walk is a bit confusing terminology, since k is usually chosen such that the jump and the walk take the same time; it does not really match the intuitive idea of the relative speed of a jumper and a walker.

$O(k^{-1/d})$. Therefore, taking $k = \mathcal{F}(\mathcal{T})^{1-1/(d+1)}$ balances the jump and the walk costs. Another remark is that if the landmarks are a random subset of the vertices of \mathcal{T} (as is the classical Jump & Walk), then the cost of the walk is $\mathcal{F}(n/k)$ [8, Variation of Lemma 4]. Assuming $\mathcal{F}(j) = O(j^\beta)$, the jump and the walk costs are balanced by taking $k = n^{1-1/(\beta+1)}$ in this case.

If Conjecture 1 is verified, constructing Delaunay triangulation using Jump & Walk for surface reconstruction purpose should use a sample of size $O(n^{1/3})$ and not $O(n^{1/4})$ as for random points in 3D; this is verified experimentally in Section 6.

Walk & Walk. In Walk & Walk, the data structure to store the landmarks is a Delaunay triangulation \mathcal{L} , in which it is possible to walk (notice that \mathcal{T} may not be a Delaunay triangulation). Assuming a random order on the landmarks, inserting or deleting a landmark after location takes $Q(k) = O(1)$ and jump step takes $J(k) = O(\mathcal{F}(\mathcal{L}))$.

If the queries and the sites are both evenly distributed we get $J(k) = O(k^{1/d})$ and $|ql_q| \cdot \mathcal{F}(\mathcal{T}) = O(k^{-1/d} \cdot n^{1/d})$ which gives $k = \sqrt{n}$ to balance the jump and walk costs. Finally, the point location takes expected time $O(n^{1/2d})$.

If walking inside \mathcal{T} and \mathcal{L} takes linear time, $k = n^{1-1/(d+1)}$ balances Walk & Walk costs.

Delaunay Hierarchy of Queries. A natural idea is to use several layers of triangulations, walking at each level from the location at the one above. When the landmarks are vertices of \mathcal{T} and each sample takes a constant ratio of the vertices at the level below, this idea yields the Delaunay hierarchy [8].

Storing the queries in a Delaunay hierarchy may have some interesting effects: if \mathcal{T} has some bad behavior $\mathcal{F}(\mathcal{T}) \gg n^{1/d}$ and there is many well-distributed queries, we can get interesting query time to the price of polynomial storage. More precisely, if the queries are such that a random sample of the queries has a Delaunay triangulation of expected linear size (always true in 2D), then using a random sample of k queries for the landmarks and a Delaunay hierarchy to store \mathcal{L} gives $Q(k) = J(k) = O(\log k)$. Then by Theorem 2 we have $|ql_q| = O(k^{-1/d})$ (amortized) and taking $k = \mathcal{F}(\mathcal{T})^d / \log^d n$ balances jump and walk costs giving a logarithmic location time.

5 Climbing up in the Delaunay Hierarchy

Up to now, the aim was to choose a good starting point to walk in \mathcal{T} . In this section, we show how a good starting point can be used within the Delaunay hierarchy to improve point location. Assume \mathcal{T} is a Delaunay triangulation, then classical use of the Delaunay hierarchy provides a logarithmic cost in the total size of \mathcal{T} to locate a point. The cost we reach here is logarithmic in the local complexity of the triangulation, that is logarithmic in the number of vertices of \mathcal{T} *in between* the starting point and the query.

Given a set of n points \mathcal{P} in the plane, the Delaunay hierarchy [8] constructs random samples $\mathcal{P} = \mathcal{P}_0 \subset \mathcal{P}_1 \subset \mathcal{P}_2 \subset \dots \subset \mathcal{P}_h$ such that $Prob(p \in \mathcal{P}_{i+1} | p \in \mathcal{P}_i) = 1/\alpha$ for some constant $\alpha > 1$. The $h+1$ Delaunay triangulations \mathcal{D}_i of \mathcal{P}_i are computed and the hierarchy is used to find the nearest-neighbor of a query q by walking at one level i from the nearest-neighbor of q at the level $i+1$. It

is proven that the expected cost of walking at one level is $O(\alpha)$ and since the expected number of levels is $\log_\alpha n$, we obtain a logarithmic expected time to descend the hierarchy for point location.

If a good starting vertex $v = v_0$ in \mathcal{D}_0 is known, the Delaunay hierarchy can be used in another way: from v_0 a walk starts in \mathcal{D}_0 visiting simplices crossed by segment v_0q ; the walk is stopped, either if the simplex containing q is found, or if a simplex having a vertex v_1 belonging to the sample \mathcal{P}_1 is found. If the walk stops because v_1 is found, then a new walk in \mathcal{D}_1 starts at v_1 along segment v_1q . This process continues recursively up to the level l where a simplex of \mathcal{D}_l that contains q is found. Finally, the hierarchy is descended as in the usual point location.

Theorem 17. *Given a set of n points \mathcal{P} such that the Delaunay triangulation of a random sample of size r of \mathcal{P} satisfies the Distribution Condition with $\mathcal{F}(r)$ polynomial, then the expected cost of climbing and descending the Delaunay hierarchy from a vertex v to a query point q is $O(\log w)$ where w is the cost of the walk from v to q in \mathcal{D} the Delaunay triangulation of \mathcal{P} .*

Proof. Climbing one level. Since the probability that any vertex of \mathcal{D}_i belongs to \mathcal{D}_{i+1} is $1/\alpha$, and that each time a new simplex is visited during the walk, a new vertex is discovered, the expected number of visited simplices before the detection of a vertex that belongs to \mathcal{D}_{i+1} is $1 + \sum_{j=0}^{\infty} j \frac{1}{\alpha} \left(1 - \frac{1}{\alpha}\right)^j = \alpha$.

Descending one level. The cost of descending one level is $O(\alpha)$ [8, Lemma 4].

Number of levels. Let w_i denote the number of edges crossed by v_iq in \mathcal{D}_i ; the Distribution Condition gives $w_i = \mathcal{F}(n/\alpha^i)|v_iq| \leq \mathcal{F}(n/\alpha^i)|v_0q|$. If $\mathcal{F}(r)$ is a polynomial function $O(r^\beta)$, the expected number of levels that we climb before descending is less than $l = (\log w_0)/\beta$ since we have

$$w_l = \mathcal{F}(n/\alpha^l)|v_lq| \leq \mathcal{F}(n/\alpha^l)|v_0q| = w_0/\alpha^{l\beta} = w_0/\alpha^{\log w_0} = 1$$

(where the big O have been omitted). Thus at level l the walk takes constant time. \square

6 Experimental Results

Experiments² have been realized on synthetic and realistic models³ (scaled to fit in the unit cube).

6.1 The Distribution Condition

Our first set of experiments is an experimental verification of the Distribution Condition. We compute the Delaunay triangulation of different inputs, either artificial or realistic, with several sizes; for realistic inputs we construct files of various sizes by taking random samples of the desired size.

² The hardware used for the experiments described in the sequel is a MacBook Pro 3,1 equipped with an 2.6 GHz Intel Core 2 processor and 2 GB 667 MHz DDR2 SDRAM, Mac OS X version 10.5.7. The software uses CGAL 3.5 [5] and is compiled with `g++ 4.3.2` and options `-O3 -DNDEBUG`.

³The scanned models used here: Pooran's Hand and Galaad, are taken from Aim@shape repository.

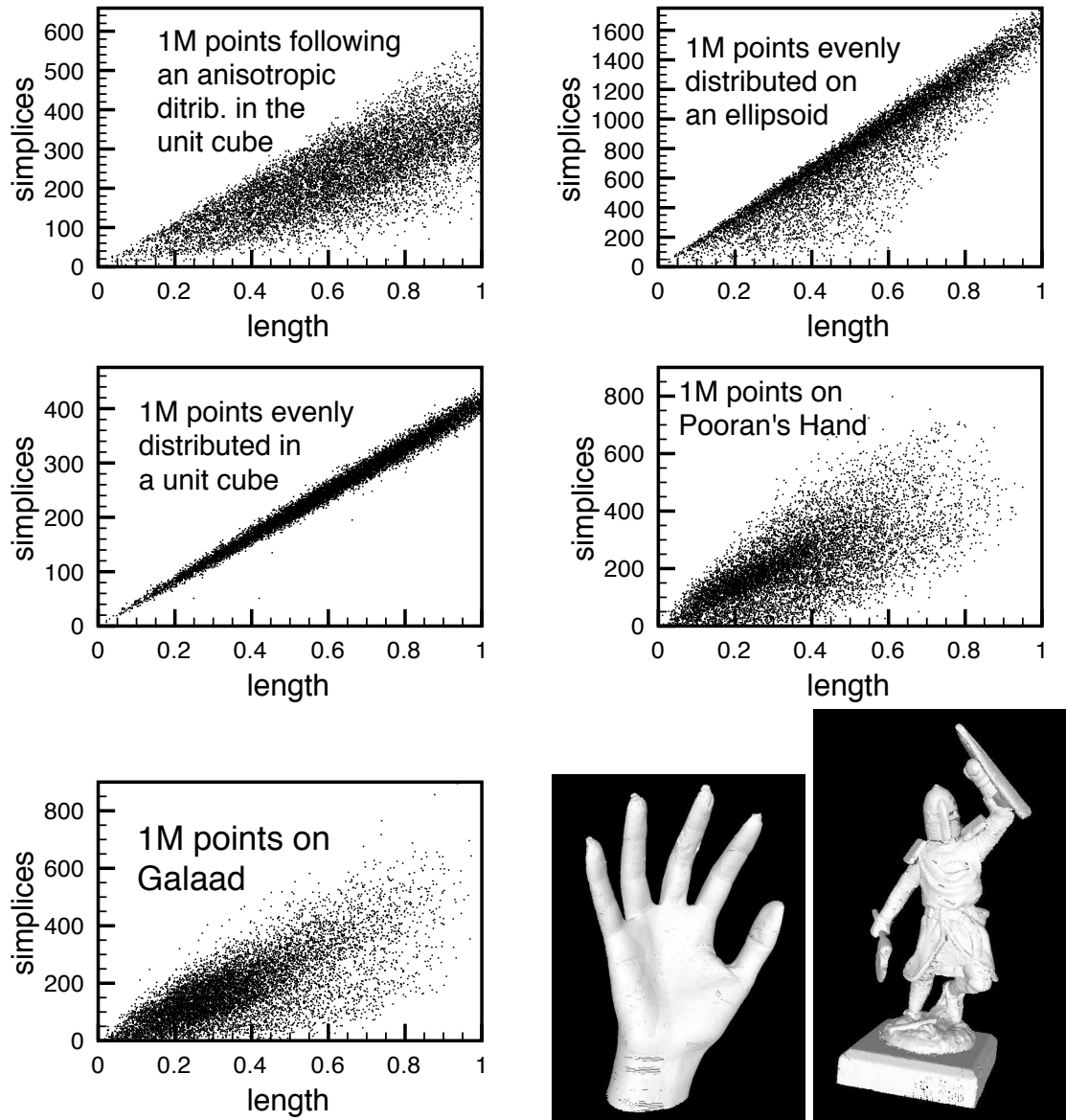


Figure 4: **Distribution condition.** $\#$ of crossed tetrahedra in terms of the length of the walk.

We consider several data sets in 3D:

- points distributed in a cube with random uniform distribution,
- points distributed in a cube with a $\rho = x^2$ density,
- points distributed on the surface of an ellipsoid with random uniform distribution, the lengths of the ellipsoid axes are $1/3$, $2/3$, and 1 ,
- Pooran’s Hand is a data set obtained by scanning a 3D model of a Hand, and
- Galaad is a data set obtained by scanning a 3D model of a toy soldier.

Files of different sizes, smaller than the original model are obtained by taking random samples of the main file with the desired number of points.

Pooran’s Hand and Galaad are originally defined in a parallelepiped much bigger than $[0, 1]^3$. We scaled each axis by the same factor and translated so to have these models constrict inside $[0, 1]^3$.

Figure 4 shows the number of simplices crossed by the walk in terms of the length of the walk, for various, randomly chosen, walks in the triangulation. Notice that even if there is some dispersion in the result, the dispersion is much more below than above the clouds of points. This is a very good news because it means that you more likely to go faster than slower compared to the expected behavior.

From that picture, the slope of lines through these points give $\mathcal{F}(\mathcal{T})$, then we draw $\mathcal{F}(\mathcal{T})$ in terms of the triangulation size in Figure 5; the slope of the different curves gives the exponent of n . The points sampled on an ellipsoid give $\log \mathcal{F}(n) \sim 0.52$ which is not far from Conjecture 1 that claims $\mathcal{F}(n) = O(n^{1/2})$. The points evenly distributed in a cube gives $\log \mathcal{F}(n) \sim 0.31$, which is not far from $\mathcal{F}(n) = O(n^{1/3})$.

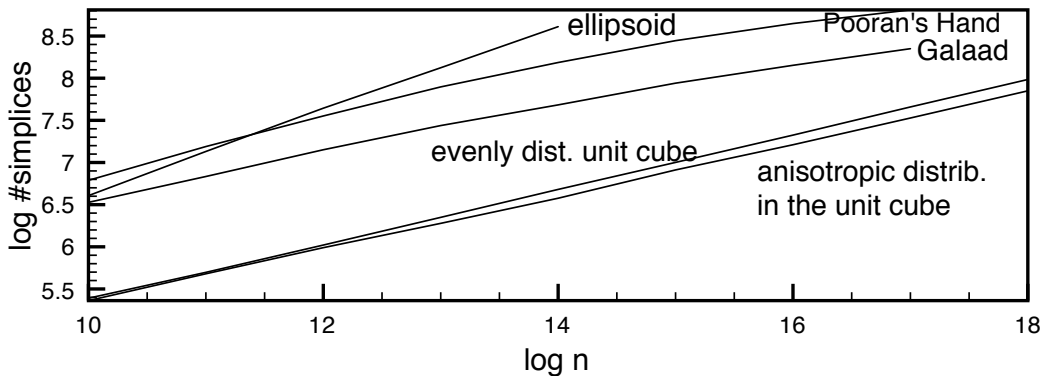


Figure 5: **Distribution condition.** Assuming $\mathcal{F}(n) = n^\alpha$, α is given by the slope of above “lines” (log here is \log_2).

6.2 k -last-points strategy

CGAL library [18] uses spatial sorting [6] to introduce a strong spatial coherence in a set of points. For several models, we locate $1M$ queries evenly distributed inside the model with the k -last-point strategy after a spatial sorting of the queries. Surprisingly, using a small k slightly improves on $k = 1$ which indicates that even with such a strong coherence, k -last-points strategy is relevant. Fig-

ure 6 shows the running times on various sets for different values of k , taking $k = 4$ always improves on $k = 1$ and in some cases by a substantial amount.

k	1	2	3	4	5	6	$k = 4$ improves on $k = 1$ by
2D							
uniform square	1.70	1.65	1.65	1.65	1.66	1.67	2%
anisotropic square	1.64	1.61	1.60	1.60	1.61	1.62	1%
ellipse	3.07	2.73	2.62	2.56	2.54	2.52	17%
3D							
uniform cube	3.57	3.45	3.41	3.39	3.40	3.46	5%
anisotropic cube	3.45	3.35	3.32	3.31	3.32	3.39	4%
ellipsoid	6.34	5.71	5.48	5.38	5.34	5.44	15%
Pooran's Hand	3.81	3.63	3.58	3.57	3.56	3.63	6%
Galaad	4.19	4.08	4.04	4.03	4.07	4.12	3%

Figure 6: **Static point location with space-filling heuristic plus k -last-points strategy.**

6.3 Self adapting point location

Now, we compare the performance of classical Jump & Walk, Delaunay hierarchy, last-point strategy and Keep, Jump, & Walk. For this purpose we consider the following experiment scenario. Let \mathcal{M} be a scanned model with $1M$ points inside the unit cube, and \mathcal{B}_r be a ball centered at $(0.5, 0.5, 0.5)$ with radius r . Now define S_n as the set of n points on the surface of the model enclosed by \mathcal{B}_r . Take values of r such that $n = n_i = 2^i$, for $i = 14, 15, \dots, 20$. Now form the sequence A_i of $1M$ points taken randomly from S_{n_i} and slightly perturbed (as to avoid arithmetic filter failures). Figure 7 shows the computation times for point location for the different strategies in function of $\log_2 n_i$.

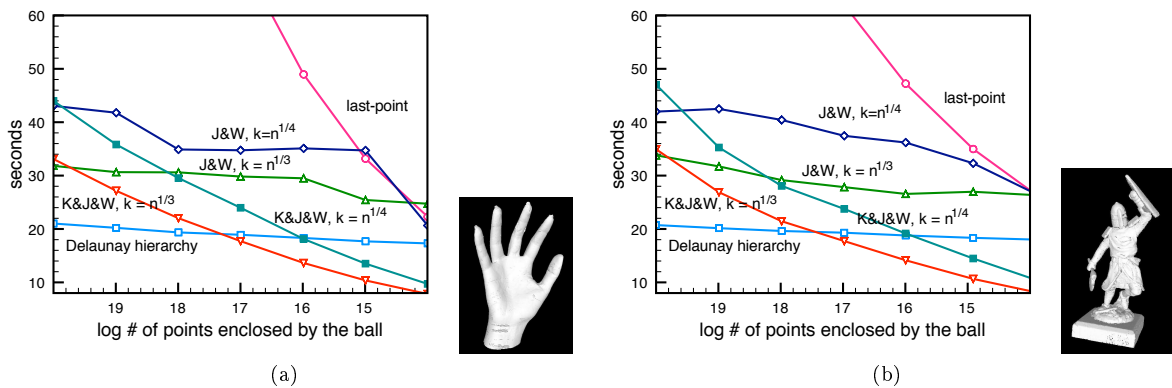


Figure 7: **Performance on a dynamic setting.** *Computation times of the various algorithms in function of the number of points on the model enclosed by a ball centered at $(0.5, 0.5, 0.5)$ for: (a) Pooran's Hand model; and (b) Galaad model.*

In both models, Keep, Jump, & Walk becomes quickly faster than Jump & Walk when the locality of the queries is stronger. More precisely, this happens when

the ball encloses less than $512k$ points in any case. Also, Keep, Jump, & Walk becomes faster than the Delaunay hierarchy when the ball encloses less than $64k$ points. These quantities of points could be multiplied by 2 if instead of picking $\sqrt[4]{n}$ landmarks we pick $\sqrt[3]{n}$ landmarks (which is in accord with Conjecture 1, see Section 4). As the number of points enclosed by the ball decreases, Keep, Jump, & Walk improves its performance, and becomes twice faster than the Delaunay hierarchy. The classical Jump & Walk cannot perform better than the Delaunay hierarchy on such big examples.

Now consider the sequence A' formed by ordering points in S_{1M} on a space-filling curve. Now A' has a strong spatial coherence. This situation is slightly different from Section 6.2, here the queries are close to the model boundary, while in Section 6.2 they were inside the model. Table 8 shows the performance of the different strategies to locate sequential queries in A' for Pooran's Hand model and Galaad model.

Models	last-point	J&W, $k = \sqrt[4]{n} = 32$	J&W, $k = \sqrt[3]{n} = 101$
Pooran's Hand	3.86	25.73	20.01
Galaad	3.91	28.41	21.62
	Delaunay hierarchy	K,J,&W, $k = \sqrt[4]{n} = 32$	K,J,&W, $k = \sqrt[3]{n} = 101$
Pooran's Hand	15.14	3.49	4.30
Galaad	16.44	3.49	4.27

Figure 8: **Performance on a static setting.** *Queries close to the model boundary are ordered as to appear in sequence on a space-filling curve. The table shows the computation time to locate the whole sequence of points with different strategies.*

Taking $k = \sqrt[4]{n} = 32$ makes Keep, Jump, & Walk faster than the last-point strategy even though S' has a strong spatial coherence.

7 Conclusion

This work discussed how the Distribution Condition and the length of some trees embedded in \mathbb{R}^d can be put together to explain self-adapting variants of well-known algorithms for point location. In the case of query-points with no spatial coherence this works showed that the constant involved with self-adapting strategies, such as the last-point strategy, is not that bad for evenly distributed points. In particular, Keep, Jump, & Walk has the same computational complexity than Jump & Walk if we use a brute-force nearest neighbor search approach. This work also provides experimental evidences that: (i) realistic data-sets satisfy the Distribution Condition; and (ii) self-adapting variant of the Jump & Walk is rather likely to improve performance, than decrease it, in both static and dynamic settings.

Designing a point location data structure to retrieve queries in a time logarithmic in the local complexity, without any hypotheses, is a very delicate question [7]. As long as the triangulation satisfies some hypotheses, we showed a simple data structure which achieves this complexity. The good points here are three: (i) the Delaunay hierarchy is simple and has a good practical behavior [8] (it is currently implemented in CGAL) (ii) the pre-processing and memory complexity are strictly better than previous data structures [15, 7] (which in

the other hand work for general planar triangulation), (iii) the proposed point location algorithm generalizes for any finite dimension.

Acknowledgments The authors wish to thank Aim@shape for providing the realistic models.

References

- [1] Pierre Alliez, Laurent Saboret, and Nader Salman. Point set processing. In CGAL Editorial Board, editor, *CGAL User and Reference Manual*. 3.5 edition, 2009. http://www.cgal.org/Manual/3.5/doc_html/cgal_manual/packages.html#Pkg:PointSetProcessing
- [2] Sunil Arya, Theocharis Malamatos, and David M. Mount. A simple entropy-based algorithm for planar point location. *ACM Trans. Algorithms*, 3(2):17, 2007.
- [3] D. H. Bailey, J. M. Borwein, and R. E. Crandall. Box integrals. *J. Comput. Appl. Math.*, 206(1):196–208, 2007.
- [4] J. Beardwood, J. H. Halton, and J. M. Hammersley. The shortest path through many points. *Math. Proc. Camb. Phil. Soc.*, 55:299–327, 1959.
- [5] CGAL Editorial Board. *CGAL User and Reference Manual*, 3.5 edition, 2009. http://www.cgal.org/Manual/3.5/doc_html/cgal_manual/packages.html.
- [6] Christophe Delage. Spatial sorting. In CGAL Editorial Board, editor, *CGAL User and Reference Manual*. 3.5 edition, 2009. http://www.cgal.org/Manual/3.5/doc_html/cgal_manual/packages.html#Pkg:SpatialSorting.
- [7] Erik D. Demaine, John Iacono, and Stefan Langerman. Proximate point searching. *Comput. Geom. Theory Appl.*, 28(1):29–40, 2004.
- [8] Olivier Devillers. The Delaunay hierarchy. *Internat. J. Found. Comput. Sci.*, 13:163–180, 2002.
- [9] Olivier Devillers, Sylvain Pion, and Monique Teillaud. Walking in a triangulation. *Internat. J. Found. Comput. Sci.*, 13:181–199, 2002.
- [10] Luc Devroye, Christophe Lemaire, and Jean-Michel Moreau. Expected time analysis for Delaunay point location. *Comput. Geom. Theory Appl.*, 29:61–89, 2004.
- [11] Luc Devroye, Ernst Peter Mücke, and Binhai Zhu. A note on point location in Delaunay triangulations of random points. *Algorithmica*, 22:477–482, 1998.
- [12] J. Gao and J. M. Steele. General spacefilling curve heuristics and limit theory for the traveling salesman problem. *Journal of Complexity*, 10:230–245, 1994.
- [13] J. E. Goodman and J. O’Rourke, editors. *Handbook of Discrete and Computational Geometry*. CRC Press LLC, Boca Raton, FL, 2004. 2nd edition.

-
- [14] John Iacono. Expected asymptotically optimal planar point location. *Comput. Geom. Theory Appl.*, 29(1):19–22, 2004.
 - [15] John Iacono and Stefan Langerman. Proximate planar point location. In *Proc. 19th Annu. Symp. Comp. Geom.*, pages 220–226, 2003.
 - [16] D. G. Kirkpatrick. Optimal search in planar subdivisions. *SIAM J. Comput.*, 12(1):28–35, 1983.
 - [17] Ernst P. Mücke, Isaac Saias, and Binhai Zhu. Fast randomized point location without preprocessing in two- and three-dimensional Delaunay triangulations. In *Proc. 12th Annu. Sympos. Comput. Geom.*, pages 274–283, 1996.
 - [18] Sylvain Pion and Monique Teillaud. 3D triangulations. In CGAL Editorial Board, editor, *CGAL User and Reference Manual*. 3.5 edition, 2009. http://www.cgal.org/Manual/3.5/doc_html/cgal_manual/packages.html#Pkg:Triangulation3.
 - [19] L. K. Platzman and J. J. Bartholdi, III. Spacefilling curves and the planar travelling salesman problem. *J. ACM*, 36(4):719–737, October 1989.
 - [20] Anderssen R., R. Brent, D. Daley, and P. Moran. Concerning $\int_0^1 \dots \int_0^1 \sqrt{x_1^2 + \dots + x_k^2} dx_1 \dots dx_k$ and a Taylor Series Method. *SIAM J. Appl. Math.*, 30:22–30, 1976.
 - [21] Luis A. Santaló. *Integral Geometry and Geometric Probability*. Addison-Wesley, 1976.
 - [22] Steven S. Skiena. *The Algorithm Design Manual*. Springer, 2008.
 - [23] J. M. Steele. Cost of sequential connection for points in space. *Operations Research Letters*, 8:137–142, 1989.
 - [24] J. M. Steele and T. L. Snyder. Worst-case growth rates of some classical problems of combinatorial optimization. *SIAM J. Comput.*, 18:278–287, 1989.



Centre de recherche INRIA Sophia Antipolis – Méditerranée
2004, route des Lucioles - BP 93 - 06902 Sophia Antipolis Cedex (France)

Centre de recherche INRIA Bordeaux – Sud Ouest : Domaine Universitaire - 351, cours de la Libération - 33405 Talence Cedex
Centre de recherche INRIA Grenoble – Rhône-Alpes : 655, avenue de l'Europe - 38334 Montbonnot Saint-Ismier
Centre de recherche INRIA Lille – Nord Europe : Parc Scientifique de la Haute Borne - 40, avenue Halley - 59650 Villeneuve d'Ascq
Centre de recherche INRIA Nancy – Grand Est : LORIA, Technopôle de Nancy-Brabois - Campus scientifique
615, rue du Jardin Botanique - BP 101 - 54602 Villers-lès-Nancy Cedex
Centre de recherche INRIA Paris – Rocquencourt : Domaine de Voluceau - Rocquencourt - BP 105 - 78153 Le Chesnay Cedex
Centre de recherche INRIA Rennes – Bretagne Atlantique : IRISA, Campus universitaire de Beaulieu - 35042 Rennes Cedex
Centre de recherche INRIA Saclay – Île-de-France : Parc Orsay Université - ZAC des Vignes : 4, rue Jacques Monod - 91893 Orsay Cedex

Éditeur
INRIA - Domaine de Voluceau - Rocquencourt, BP 105 - 78153 Le Chesnay Cedex (France)
<http://www.inria.fr>
ISSN 0249-6399